

## Materials and Manufacturing Processes

Publication details, including instructions for authors and subscription information:

<http://www.tandfonline.com/loi/lmmp20>

### Experimental Investigation of Underwater Stud Friction Stir Welding Parameters

R. M. Chandima Ratnayake<sup>a</sup> & V. A. Brevik<sup>a</sup>

<sup>a</sup> Department of Mechanical and Structural Engineering and Materials Science , University of Stavanger , Stavanger , Norway

Accepted author version posted online: 02 Jul 2014. Published online: 10 Sep 2014.

To cite this article: R. M. Chandima Ratnayake & V. A. Brevik (2014) Experimental Investigation of Underwater Stud Friction Stir Welding Parameters, Materials and Manufacturing Processes, 29:10, 1219-1225, DOI: [10.1080/10426914.2014.930891](https://doi.org/10.1080/10426914.2014.930891)

To link to this article: <http://dx.doi.org/10.1080/10426914.2014.930891>

PLEASE SCROLL DOWN FOR ARTICLE

Taylor & Francis makes every effort to ensure the accuracy of all the information (the "Content") contained in the publications on our platform. However, Taylor & Francis, our agents, and our licensors make no representations or warranties whatsoever as to the accuracy, completeness, or suitability for any purpose of the Content. Any opinions and views expressed in this publication are the opinions and views of the authors, and are not the views of or endorsed by Taylor & Francis. The accuracy of the Content should not be relied upon and should be independently verified with primary sources of information. Taylor and Francis shall not be liable for any losses, actions, claims, proceedings, demands, costs, expenses, damages, and other liabilities whatsoever or howsoever caused arising directly or indirectly in connection with, in relation to or arising out of the use of the Content.

This article may be used for research, teaching, and private study purposes. Any substantial or systematic reproduction, redistribution, reselling, loan, sub-licensing, systematic supply, or distribution in any form to anyone is expressly forbidden. Terms & Conditions of access and use can be found at <http://www.tandfonline.com/page/terms-and-conditions>

# Experimental Investigation of Underwater Stud Friction Stir Welding Parameters

R. M. CHANDIMA RATNAYAKE AND V. A. BREVIK

*Department of Mechanical and Structural Engineering and Materials Science, University of Stavanger, Stavanger, Norway*

Optimum parameter settings for stud friction stir welding (SFSW) in underwater conditions are experimentally investigated using M12 electrical galvanized bolts of grade 8.8 and plates of S235 (St37) steel. Several sets of SFSW experiments in underwater conditions are performed without a shroud to investigate the approximate input parameter (i.e., speed, pressure, heating time, and upset) interactions. The tensile strength of each stud weld is measured to investigate welded joint performance. The pressure ranges and corresponding speeds which produce consistent strength levels are identified. Further experimentation is performed within the selected pressure ranges to investigate the variation of tensile strength. The upset is also measured as an output performance factor. The microstructure is examined to observe different regions. Hardness is measured at each region to investigate the martensite formation.

**Keywords** Experiment; Friction; Pressure; Speed; Stud; Underwater; Upset; Welding.

## INTRODUCTION

Mitelea et al. [1] and Liu et al. [2] revealed that friction welding has become a highly productive process, with significant importance in underwater conditions, since it requires short processing times (i.e., from a fraction of a second to several seconds) and leads to the fabrication of reliable welded joints. Liu et al. [3], Johnsen [4], Joelj [5], Mishra, and Ma [6] showed that, as friction stir welding (FSW) is a solid state joining process, it has been widely utilized to construct welded joints that were difficult to make using fusion welds. Liu et al. [3] and Johnsen [4] discovered that thermal cycles applied to the FSW samples reduced the mechanical properties of the joints (i.e., the joint's tensile strength becomes weaker than that of the base material), although the low heat input generated during FSW does not lead to the melting of the base metal. Zhang et al. [7] reported the possibility of improving the strength of normal FSW joints by accelerating the heat dissipation. They explored the temperature histories of underwater FSW, in which the whole work piece was kept immersed in water during the welding. Xue et al. [8] reported the prospect of recognizing three distinct zones (i.e., the stirred zone, thermo-mechanically affected zone, and heat-affected zone (HAZ)) based on microstructural characterization in the FSW joints.

Fratini et al. [9] experimented with the in-process heat treatment, having water flowing on the top surface of the

samples during FSW, and their results indicated that the tensile strength of the joints was improved by the cooling action. Liu et al. [2, 3] proposed and experimented with underwater FSW to obtain the full advantage of the heat absorption effect of water. Liu et al. [3] compared the mechanical properties of 2219 aluminum alloy FSW joints in air and under water. Upadhyay and Reynolds [10] researched the effect of thermal boundaries on friction stir welded 7050-T7 aluminum alloy sheets. Their experiments revealed that the surface convection in submerged FSW was higher, thus resulting in a decrease in the tool temperature and an increase in the torque required (i.e., alternatively an increase in power consumption). Upadhyay and Reynolds's results [10] also indicated that the hardness of the submerged weld nugget was higher than that of the FSW in air. Hofmann and Vecchio [11] studied the effect of submerging friction stir processing on a grain size of aluminum alloy Al-6061-T6 compared to FSP in air. The results of aforementioned study indicated that more grain refinement was attained under submerging conditions due to the faster cooling rate. Hofmann and Vecchio [11] also used a boundary migration model to predict the grain size using measured thermal histories of the stirred material. Darras and Kishta [12] reported that a limited number of studies had investigated submerged friction stirring. Liu et al. [3] proved that

the tensile strength of the underwater joint was significantly higher than that of the normal joint, confirming feasibility of underwater FSW to improve mechanical properties of the normal joints. Although external water cooling has been demonstrated to be available for the strength improvement in the previous studies, the relationship between the process variables and the performance of the cooled joint has not yet been developed. [2]

Received March 16, 2014; Accepted May 7, 2014

Address correspondence to R. M. Chandima Ratnayake, Department of Mechanical and Structural Engineering and Materials Science, University of Stavanger, N-4036 Stavanger, Norway; E-mail: chandima.ratnayake@uis.no

Color versions of one or more of the figures in the article can be found online at [www.tandfonline.com/lmmp](http://www.tandfonline.com/lmmp).

A limited number of studies were conducted in the field of underwater FSW to investigate the relationship between the process variables and the performance of the welded joint. Therefore, grade 8.8 bolts (where the heads of each bolt have been cut off to make studs for performing the experiments) and S235 structural steel plates were underwater friction stir welded in the present study and the effect of welding speed and pressure on the joint quality was investigated, presented, and discussed in relation to microstructures, hardness distributions, and mechanical (tensile strength) properties.

#### PRACTICAL SIGNIFICANCE

The friction welding processes are generally sensitive to the surroundings in which they are conducted [13, 14]. For instance, underwater FSW causes rapid cooling of the weld in the North Sea underwater environments [15]. For instance, practical experience, research, and literature indicate that when the steel studs are friction welded to steel plates, the quenching effect gives rise to excessive hardness and severe cracking even at relatively shallow depths [15]. Although the cooling efficiency of the water is supposed to be independent of depth, there are slight changes due to the variation of temperature and salinity [16, 17]. The aforementioned becomes a significant challenge, especially in the case of subsea interventions for modifications and repair activities using friction welding in the North Sea. For instance, friction stud welding has been “utilized to retrofit sacrificial anodes to subsea pipelines although the pipeline is live (that is, it proceeds to transportation hydrocarbons at pressure)” [18]. In some instances the anodes are positioned on the sea bed “next to the pipeline and a lug on a cable from the anode is connected to the stud welded on the pipeline” [18]. However, the effect of cooling rates due to the surrounding water is mitigated by the foamed plastics which are utilized to form a shroud around the weld region [19]. In essence, a shroud protects the friction welded joint from the surrounding water during the FSW, minimizing the quenching effect (i.e., minimized hardness changes) and giving acceptable

welds [20]. However, some of the tailor-made SFSW applications demand that they are performed without a shroud. It is a challenge to estimate optimum stud FSW parameter settings, under no shroud conditions, which meet the optimal strength requirements. Hence, the aforementioned kind of applications requires the determination of those parameter settings which provide optimal strength and material property requirements in a friction welded joint. The experiment performed in this study focuses on a special case, in which a tailor-made SFSW design is going to be integrated with a remotely operated underwater vehicle and perform the stud FSW without using a shroud. The article provides the results of the experimental SFSW study performed in underwater conditions without utilizing a shroud in order to investigate optimum parameter settings.

#### METHODOLOGY

##### *Design of the Stud FSW Test Rig*

First, a model of a stud FSW test rig was designed and animated using solid edge to observe its performance. After that a prototype of the designed test model was fabricated (see Fig. 1(a)). The lever arm has been calibrated in relation to different load requirements.

Figure 1(b) illustrates the arrangement to hold the plate and stud inside a container during FSW to immerse the welding zone (i.e., to make submerged or subsea conditions). The water container allows the welding area to be surrounded by salt water to create actual conditions consisting of 35 g of sea salt per liter. The plastic rim around the welding area could contain about a half liter of water and the SFSW performed in about 6–7 cm underwater. The test was performed using partially threaded M12 electrical galvanized bolts of grade 8.8 and plates of S235 (St37) steel (see Table 1).

The studs were prepared by cutting the heads off, leaving a remaining length of about 48 mm, ensuring that the threads shall not interfere with the weld (i.e., about 10 mm of unthreaded bolt stem at the bottom along the vertical axis). Each stud was held in place by simply screwing it into the motor coupling (see Fig. 2).

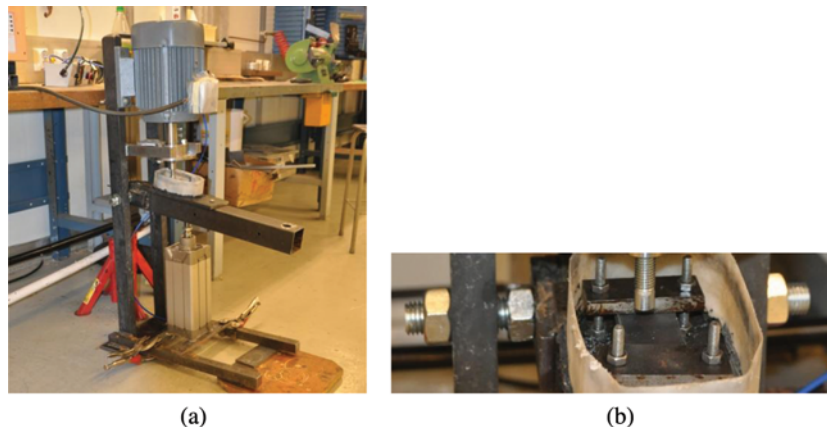


FIGURE 1.—(a) Prototype of the FRSW test rig and (b) a container to immerse the welding zone.

TABLE 1.—Details of plate and stud.

Steel	S235	Class 8.8 bolt
C	0.17 max	0.25–0.55
Mn	1.40 max	NA
P	0.035 max	0.04 max
S	0.035 max	0.05 max
Cu	0.55 max	NA
N	0.012 max	NA
Heat treatment	Hot rolled	Quenched and tempered
Minimum yield strength	235 MPa	640 MPa
Minimum tensile strength	363 MPa	800 MPa
Minimum elongation	23%	12%

Plates with 10 mm thickness have been cut to about (30 × 100) mm pieces and tightened to the test rig (see Fig. 2). As the electric motors are not designed to meet high axial loads on the shaft, a supportive thrust bearing has been placed to take the axial load during SFSW. This has also been designed to enable increased stability for the specimen and maintain its alignment with the motor shaft axis during welding. In order to cope with the capacity of the existing pneumatic cylinder, a lever arm has been introduced to the SFSW test rig, meeting a range of required axial pressures (see Fig. 1(a)). In essence, rotational speed generated by the electric motor together with axial pressure generates heat, which produces a temperature increase on the joint surface sufficient for pressure welding (i.e., for steel the temperature range is between 900–1300°C). Once the temperature is reached, the relative movement of the friction surface is halted in the shortest possible time (i.e., instantaneously) to stop the introduction of heat. The SFSW process is concluded by natural cooling of the joint under the applied axial pressure [21].



FIGURE 2.—A motor coupling to hold the stud.

### Testing Approach

First, a series of tests was performed over a range of axial pressures, heating times, and speeds to investigate the approximate ranges that provide satisfactory tensile strength values at the welded joint. The *Welding Handbook* [13] published by the American Welding Society (AWS) recommends tangential velocities in the range of 250–350 feet/s (76.20–106.68 m/s) for steels. For a 12 mm specimen this gives a range of 2020–2830 rpm. The AWS *Welding Handbook* [13] also suggests heating pressures for mild steels between 30–60 MPa and forging pressures as high as 140 MPa. The same pressure was maintained during heating and forging to keep the number of welding parameters at a minimum. For instance, axial force of 11.3 kN is required to make about 100 MPa at the M12 stud. To carry out the experiment, four pressure ranges were initially selected.

### RESULTS

Pressure levels are divided into four intervals. They have been indicated using the first number of the weld, where 1 is lowest and 4 is the highest. Each weld has been given a unique number to recognize the pressure ranges based on the distance from the pivot point of the lever arm to the pneumatic cylinder. However, the actual pressure at the stud may have changed slightly due to pressure changes in air supply. Actual pressure has been calculated monitoring the air pressure and tabulated in Table 2. The speed in revolutions per minute (rpm) has been calculated based on the electric frequency monitored via a frequency converter. The motor used in the test rig limits the range of speeds to 3000–3600 rpm.

After observing all the pressure ranges, weld numbers 3.3–3.6 and 4.2–4.5 [i.e., pressure interval-3 (i.e., 90–120 MPa) and pressure interval-4 (i.e., 120–150 MPa)] were found to have fairly consistent strength levels. They have been reproduced for further verification. Table 2 illustrates the pressure ranges that are found to produce consistent strength levels based on the initial experiments.

The selected weld numbers have been further evaluated, changing the heating time to investigate potential trends related to the welding time and estimating the robustness of the parameters. Table 3 illustrates the re-evaluated results of the initially selected weld numbers.

TABLE 2.—Results of initial experimentation.

Weld No.	rpm	Pressure (MPa)	Heating time (s)	Upset (mm)	Ultimate tensile load (kN)	Tensile strength (MPa)
3.3	3000	98	3.4	4.7	33.5	296
3.4	3000	108	4.3	9.3	36.5	323
3.5	3600	108	1.9	3.6	29.7	263
3.6	3600	100	3.6	7.1	39.2	347
4.2	3000	146	2.9	7.5	42.2	373
4.3	3000	148	1.5	4.1	46.9	415
4.4	3600	133	1.2	1.8	44.1	390
4.5	3600	125	2.7	5.3	44.5	393

TABLE 3.—Re-evaluation results.

Weld No.	rpm	Pressure (MPa)	Heating time (s)	Upset (mm)	Ultimate tensile load (kN)	Tensile strength (MPa)
3.3 <sup>1</sup>	3000	111	3.3	7.4	52.0	460
3.4 <sup>1</sup>	3000	100	4.5	10.0	54.6	483
3.5 <sup>1</sup>	3600	100	1.8	2.8	32.6	288
3.6 <sup>1</sup>	3600	113	4.1	10.3	61.0	539
3.3 <sup>2</sup>	3000	98	1.6	3.0	39.6	350
3.4 <sup>2</sup>	3000	113	4.8	12.9	67.2	594
3.5 <sup>2</sup>	3600	100	3.0	5.8	43.2	382
3.6 <sup>2</sup>	3600	103	4.7	11.0	58.0	513
4.2 <sup>1</sup>	3000	129	3.2	9.2	62.2	550
4.3 <sup>1</sup>	3000	123	1.6	3.6	66.5	588
4.4 <sup>1</sup>	3600	135	1.7	4.3	57.0	504
4.5 <sup>1</sup>	3600	127	3.4	9.0	63.2	559
4.2 <sup>2</sup>	3000	135	2.3	6.3	58.0	513
4.3 <sup>2</sup>	3000	140	4.5	14.2	73.4	649
4.4 <sup>2</sup>	3600	123	1.8	4.1	65.5	580
4.5 <sup>2</sup>	3600	129	4.4	12.7	49.2	435

TABLE 4.—Average and standard deviation values for ultimate loads.

Pressure interval	Speed (rpm)	Ultimate tensile load (kN)	
		Average	Standard deviation
3	3000	52.45	8.39
3	3600	48.43	9.85
4	3000	60.25	8.49
4	3600	53.71	8.92

As it is hard to determine which speed to progress with, both the pressure intervals based on Figs. 3 and 4 and the averages and standard deviations of the ultimate load have been calculated (see Table 4) for pressure and speed combinations.

The welds at pressure intervals-3 and -4 at 3000 rpm have the lowest standard deviations. Hence, welds 3.3<sup>1</sup> and 4.2<sup>2</sup> have been selected to investigate the microstructure and hardness levels. This is also due to the fact that the strength values of these welds are at the middle of the overall strength range, having almost the same number of upset values. This selection enables the investigation of microstructural changes and hardness values under the same upset made with different heating times. Moreover, although there were welds with higher strength values (see Table 3), the main concern is for welds with strength values not significantly far from the base plate strength (i.e., 363 MPa). The observations reveal that there were no noticeable differences in the microstructure. Hence, weld 3.3<sup>1</sup> has been selected to indicate possible regions (see Fig. 5) that have been observed in all the weld cross sections in general.

To measure the hardness, a Vickers micro-hardness tester with a load of 1 kg and a load time of 10 s was

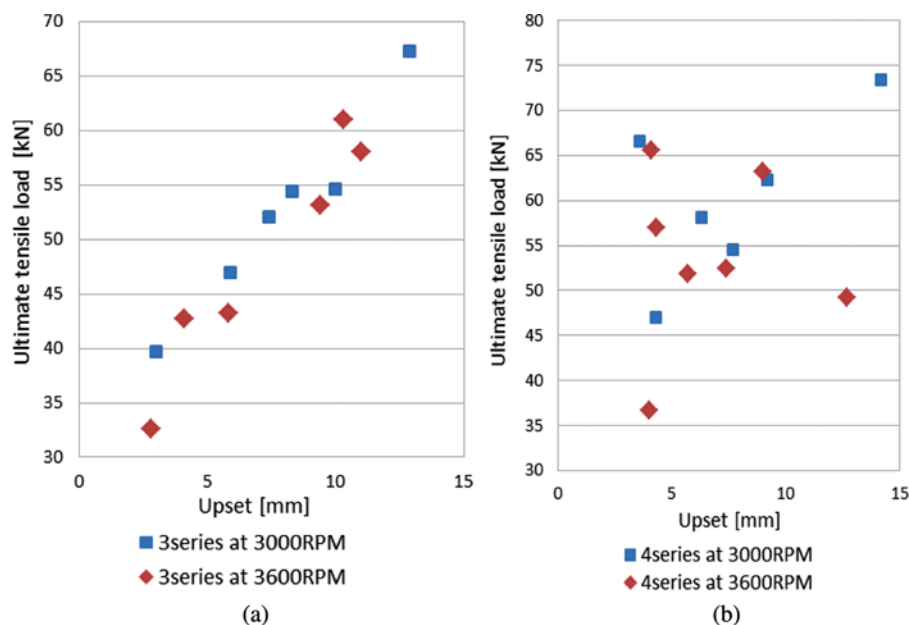


FIGURE 3.—Upset vs ultimate tensile load for the welds. (a) Made at pressure interval-3 at 3000 and 3600 rpm; (b) Made at pressure interval-4 at 3000 and 3600 rpm.



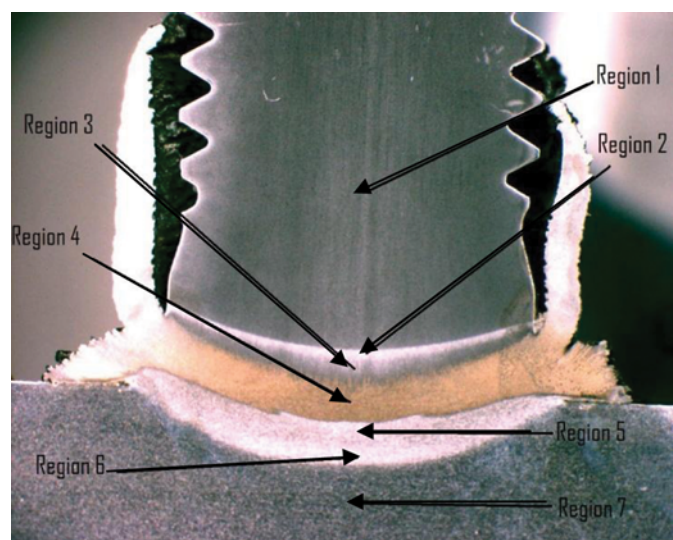


FIGURE 4.—Possible regions of FRSW number 3.3<sup>1</sup> after etching.

utilized. Figures 5–8 illustrate Regions 1–7 with approximate hardness values.

The quenched martensite structure present in Region 1 is too hard and brittle for most engineering

applications. Tempering restores some of ductility without significantly reducing the strength of the welded joint. In Region 2, the bainite structure of fine needles in a ferrite matrix is hard and has relatively low ductility.

In Region 3, the ferrite and bainite structure indicates hardness and has relatively low ductility in the welded joint. Moreover, the martensite structure present in Region 4 indicates hard and brittle characteristics in the welded joint.

Regions 5–7 indicate pearlite (i.e., usually ductile) and proeutectoid ferrite. In the areas of proeutectoid ferrite of distinctly lower hardness and strength compared to the average strength of a surfaced weld metal, deformations of the surface layer during fatigue loading bring about slip bands [22]. The number of slip bands grows along with the growth of number of cycles and these slip bands create geometric forms on the boundaries of proeutectoid grains [22]. In this context, cracks in the slip bands are important in case of fatigue cracking propagation at high stress amplitudes [22]. However, the aforementioned does not have much effect on the welded joints as they are essentially serving the purpose of fixing anodes on underwater pipelines for cathodic protection.

The welding procedure utilized in this study indicates martensite formation in the HAZ at the stud–plate

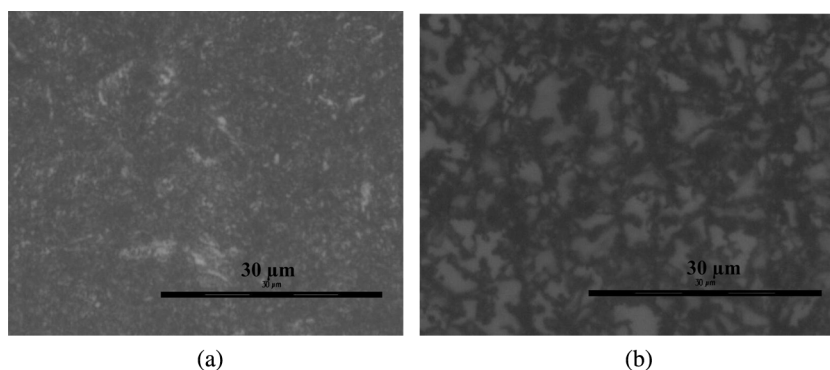


FIGURE 5.—(a) Region 1 and (b) Region 2. Region 1: Quenched and tempered martensite (base metal of the stud), 250 HV in the center, 280 HV close to the edge; Region 2: Ferrite and bainite, 240 HV in the center, 270 HV close to the edge.

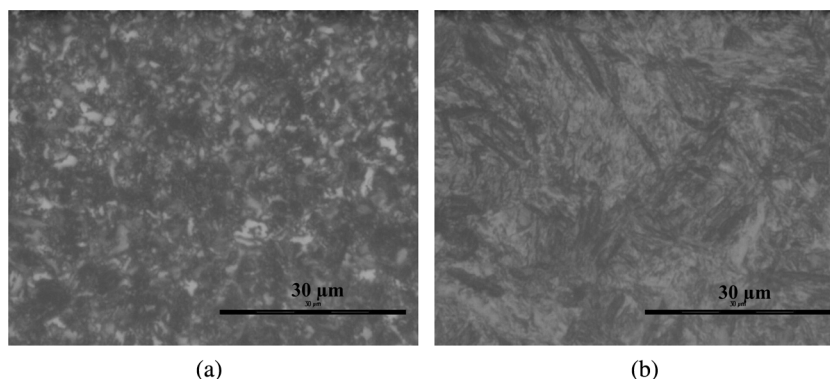


FIGURE 6.—(a) Region 3 and (b) Region 4; Region 3: Ferrite and bainite, 260 HV in the center, 280 HV close to the edge; Region 4: Martensite, 500 HV in the center, 600 HV close to the edge.

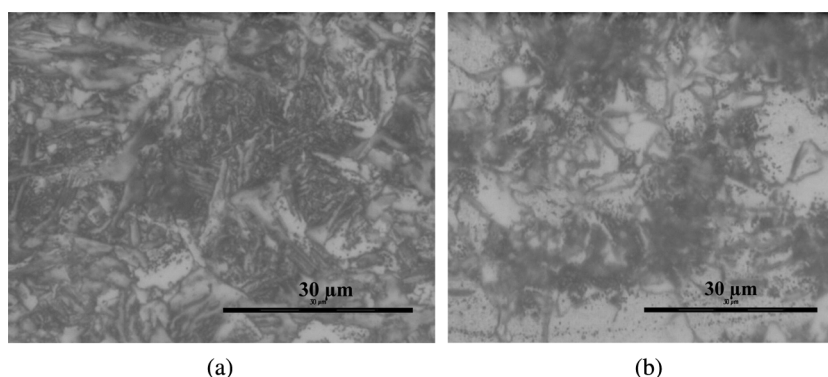


FIGURE 7.—(a) Region 5 and (b) Region 6; Region 5: Pearlite and proeutectoid ferrite, 240 HV in the center, 260 HV close to the edge; Region 6: Pearlite and proeutectoid ferrite, 220 HV at the center and edge.

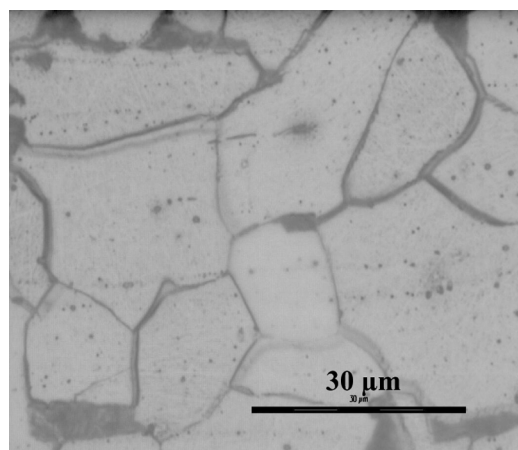


FIGURE 8.—Region 7: Proeutectoid ferrite and pearlite (base metal of the plate), 140 HV.

interface causing significantly high hardness. Microscopic examination revealed that martensite had formed in all welds at the stud–plate penetration interface.

#### CONCLUSION

Stud friction stir welds with M12 electrical galvanized bolts of grade 8.8 and plates of S235 (St37) steel have been constructed to identify the relationship between optimum strength vs pressure in underwater conditions. Joints with acceptable strength values were observed at a pressure range of 100–111 MPa, a heating time of 3.3–3.5 s, and a speed of 2900–3000 rpm. This results in upset values in the range of 6.0–7.2 mm. These parameters gave acceptable results when welding an M12 stud to a plate of S235 with 10 mm thickness. For three tensile strength tests conducted for the welds made with these parameters, the average value was 52.45 kN or 464 MPa based on the cross section of the stud.

Further research should be carried out employing an engineering robust design approach (i.e., to handle the multi-criteria nature of the optimization and to deal with inherent noise due to no shroud) to further tune the

parameters in a systematic manner. This will enable the quality of the friction stud welds to be improved (i.e., via estimating optimal parameter levels in a systematic way) by minimizing the effect of the causes of variation (i.e., without eliminating the causes) whilst they exist in the stud FSW process.

#### REFERENCES

1. Mitelea, I.; Budau, V.; Craciunescu, C. Dissimilar friction welding of induction surface-hardened steels and thermochemically treated steels. *Journal of Materials Processing Technology* **2012**, 212 (9), 1892–1899.
2. Liu, H.J.; Zhang, H.J.; Yu, L. Effect of welding speed on microstructures and mechanical properties of underwater friction stir welded 2219 aluminum alloy. *Materials & Design* **2011**, 32 (3), 1548–1553.
3. Liu, H.J.; Zhang, H.J.; Huang, Y.X.; Yu, L. Mechanical properties of underwater friction stir welded 2219 aluminum alloy. *Transactions of Nonferrous Metals Society of China* **2010**, 20 (8), 1387–1391.
4. Johnsen, M.R. Friction stir welding takes off at Boeing. *Welding Journal* **1999**, 78 (2), 35–39.
5. Joelj, D. The friction stir welding advantage. *Welding Journal* **2001**, 80 (5), 30–34.
6. Mishra, R.S.; Ma, Z.Y. Friction stir welding and processing. *Material Science and Engineering* **2005**, 50 (1/2), 1–78.
7. Zhang, H.-J.; Liu, H.-J.; Yu, L. Thermal modeling of underwater friction stir welding of high strength aluminum alloy. *Transactions of Nonferrous Metals Society of China* **2013**, 23 (4), 1114–1122.
8. Xue, P.; Xiao, B.L.; Zhang, Q.; Ma, Z.Y. Achieving friction stir welded pure copper joints with nearly equal strength to the parent metal via additional rapid cooling. *Scripta Materialia* **2011**, 64 (11), 1051–1054.
9. Fratini, L.; Buffa, G.; Shivpuri, R. In-process heat treatments to improve FS-welded butt joints. *International Journal of Advanced Manufacturing Technology* **2009**, 43, 664–670.
10. Upadhyay, P.; Reynolds, A.P. Effects of thermal boundary conditions in friction stir welded AA7050-T7 sheets. *Materials Science and Engineering A* **2010**, 157, 1537–1543.
11. Hofmann, D.C.; Vecchio, K.S. Thermal history analysis of friction stir processed and submerged friction stir processed

- aluminum. *Materials Science and Engineering A* **2007**, 465, 165–175.
12. Darras, B.; Kishta, E. Submerged friction stir processing of AZ31 Magnesium alloy. *Materials and Design* **2013**, 47, 133–137.
  13. Kearns, W. H. Welding processes – resistance and solid-state welding and other joining processes. In *Welding Handbook*, 7th Ed., Volume 3; American Welding Society: Miami, FL, 1980.
  14. TWI. Can Friction Welding be Carried Out in hostile environments? 2013. <http://www.twi.co.uk/technical-knowledge/faqs/process-faqs/faq-can-friction-welding-be-carried-out-in-hostile-environments/> (accessed October 15, 2013).
  15. Nicholas, E.D. Underwater friction welding for electrical coupling of sacrificial anodes. In *Proceedings of Offshore Technology Conference*, Houston, Texas, April 30, 1984, OTC 4741, 1984.
  16. Nikolaev, S.D.; Oskina, N.S.; Blyum, N.S.; Bubenshchikova, N.V. Neogene–Quaternary variations of the ‘Pole–Equator’ temperature gradient of the surface oceanic waters in the North Atlantic and North Pacific. *Global and Planetary Change* **1998**, 18 (3–4), 85–111.
  17. Squidoo. Friction Stud Welding. <http://www.squidoo.com/friction-stud-welding> (accessed October 15, 2013).
  18. MMM. Friction Stud Welding. <http://memcomachines.com/friction-stud-welding.aspx> (accessed October 15, 2013).
  19. Stewart, W.C. Feasibility of underwater friction stir welding of hy-80 Steel, 2011, OMB No. 0704–0188. <http://www.dtic.mil/get-tr-doc/pdf?AD=ADA543025> (accessed October 15, 2013).
  20. PROSERV. Subsea Technology – Pipeline Repair Services – Friction Stud Welding, 2013. <http://www.proserv.com/modules/xnews/article.php?storyid=862> (accessed October 15, 2013).
  21. Vill, V.I. *Friction Welding of Metals*. LCCCN 62–13420; American Welding Society, Inc.: Garfield Press, New York, USA, 1962.
  22. Rie, K.-T.; Portella, P.D. *Low Cycle Fatigue and Elastoplastic Behavior of Material*; Elsevier Science Ltd.: Oxford, UK, ISBN 008043326X, 1998; 364–366 pp.